



Trans. Nonferrous Met. Soc. China 27(2017) 2371-2380

Transactions of Nonferrous Metals Society of China

www.tnmsc.cn



Erosion and erosion—corrosion of Al-brass alloy: Effects of jet velocity, sand concentration and impingement angle on surface roughness

Morteza ABEDINI^{1,2}, Hamid M. GHASEMI¹

- 1. School of Metallurgy and Materials Engineering, College of Engineering, University of Tehran, Tehran 11155-4563, Iran;
- 2. Department of Metallurgy and Materials Engineering, University of Kashan, Kashan, Iran

Received 1 October 2016; accepted 31 December 2016

Abstract: Effects of jet velocity, sand concentration and impingement angle on the surface roughness of Al-brass alloy were investigated after erosion and erosion—corrosion tests. The tests were performed using a jet impingement rig. The eroded surfaces were characterized using 2-D and 3-D surface profilometery and scanning electron microscopy (SEM). The results showed that there was an increase in the surface roughness of the erosion—corrosion samples as sand concentration was increased to 1, 5 and 10 g/L at jet velocities of 9, 6 and 3 m/s, respectively. However, the surface roughness decreased with a further increase in sand concentration. This decrease in the surface roughness was attributed to the higher work hardening of the surface, rebounding or blanketing effect and very high frequency of the impacts at the higher sand concentrations. The surface roughness increased as the jet velocity increased. The results also showed that the change in the surface roughness with impingement angle was not significant at two jet velocities of 3 and 6 m/s. However, at a higher jet velocity of 9 m/s, formation of ripples on the erosion surfaces at oblique angles resulted in a higher surface roughness as compared with the normal impingement angle.

Key words: Al-brass; erosion-corrosion; surface topography; sand concentration

1 Introduction

Impingement of slurry on the surface of materials could damage the surfaces during the erosion-corrosion process. A single particle impact would generate a scratch or crater with raised lips on the surface [1]. This could change the surface roughness of the material, which is an important parameter in the erosion—corrosion resistance of alloys. Increasing the surface roughness would increase the corrosion rate during the erosioncorrosion process (i.e., erosion-enhanced corrosion) due to the higher effective surface area of the eroded surfaces [2]. Indeed, the increase in surface roughness through multiple particle impacts could result in formation of various micro-galvanic sites, which may increase the corrosion rate [3]. SASAKI and BURSTEIN [4] have suggested that the surface roughness generated by the erosion lowered the pitting potential, hence may be responsible for the enhanced pitting of the metal during erosion-corrosion. Surface roughness could also increase the material removal rate due to the erosion mechanisms [5]. Heat transfer, an important parameter in the heat exchanger tubes, is another important parameter that may be affected by the surface roughness [6].

ZHENG et al [7] have studied the surface roughness of 304 stainless steel and a Fe-based amorphous coating to determine the critical flow velocity during erosioncorrosion. They showed that at the velocities above the critical flow velocity, the surface roughness increased rapidly with increasing the flow velocity. Higher surface roughness of 304 stainless steel specimens at higher jet velocities and higher testing times has also been indicated by NGUYEN et al [8]. JI et al [9] have shown that the surface roughness values of the eroded surfaces were inversely related to the hardness of tested materials. The change in the surface roughness of cavitation erosion-corrosion samples was studied by RYL et al [10] using electrochemical impedance spectroscopy (EIS) technique. In another research, the lower surface roughness of Pd-Co film was considered as a reason for its lower erosion-corrosion rate as compared with Pd-Cu film [11].

Jet velocity, sand concentration and impingement

angle are the most important factors in the erosion—corrosion behaviors of materials [11,12], which could also affect the surface roughness of the eroded surfaces. To our knowledge, there have not been many studies on the effect of erosion—corrosion parameters on the surface roughness. In this work, the surface roughness of Al-brass alloy was examined after pure erosion (i.e., with cathodic protection) and erosion—corrosion tests in various conditions. The alloy has been extensively used in condensers and heat exchangers that may be exposed to the erosion—corrosion degradation [13]. The mechanisms of the change in the surface roughness of the alloy by each factor (i.e., jet velocity, sand concentration and impingement angle) were also characterized.

2 Experimental

Al-brass alloy with a composition of Cu-19.2%Zn-2.3%Al-0.1%As was melted in a resistance furnace and cast in an iron mold. The cast ingot with a thickness of 14 mm was solution annealed in a muffle furnace at 750 °C for 4 h and then cold rolled into a thickness of 8 mm. Finally, the obtained strips were annealed at 550 °C for 2 h. Erosion-corrosion samples, 5 mm in diameter and 7 mm in length, were wire-cut from the annealed strips. The erosion and erosion-corrosion surfaces, i.e., the circles at the ends of all cylindrical specimens were polished to an average roughness (R_a) of about (0.12±0.02) µm.

Erosion and erosion-corrosion tests were performed using a slurry impingement rig. The details of the rig were described elsewhere [14]. The used slurry consisted of distilled water, 35 g/L NaCl and 0-90 g/L SiO₂ particles with average size of 250-500 µm. Figure 1 shows the morphology of SiO₂ particles used in the current work. The tests were carried out under various impingement angles between 20° and 90° at three jet velocities of 3, 6 and 9 m/s for 30 min. The erosion-corrosion tests were performed at the open circuit potential (OCP). The pure erosion tests were carried out by applying a cathodic protection potential using a 302 N Autolab potentiostat/galvanostat coupled to the erosion-corrosion rig. For the pure erosion tests, the OCP of the alloy was measured in the first 60 s of each test and the voltage of specimen was then shifted -1000 mV to the obtained OCP. The counter and reference electrodes were graphite and saturated Ag/AgCl in a capillary, respectively.

The erosion and erosion-corrosion surfaces were characterized using a scanning electron microscope (SEM) equipped by an energy dispersive X-ray spectrometer (EDS). The surface roughness (R_a) of the samples was also measured using a T-8000

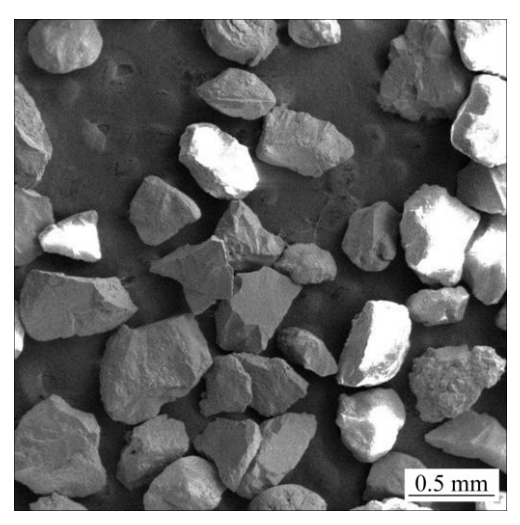


Fig. 1 SEM micrograph of eroding SiO₂ particles

Hommelwerke surface profilometer. Measurements were performed in a total length of 3 mm on the eroded surfaces using a standard cut-off length of 0.8 mm. The reported values for R_a were the average roughness of at least three measurements for each sample. The 3-D topography of some eroded surfaces was also obtained by scanning an area of 2 mm \times 2 mm of the surfaces using the surface profilometer. The distance between the line scans was set to be 10 μ m. In the case of oblique impingement angles, the roughness measurements were performed longitudinal to the particle impact direction on the eroded surfaces.

3 Results and discussion

The surface roughness of Al-brass samples after erosion and erosion-corrosion tests at three jet velocities of 3, 6 and 9 m/s as a function of particle concentration under an impingement angle of 90° is shown in Fig. 2. Almost a same trend was shown with a little change in the surface roughness for erosion (E) and erosioncorrosion (EC) samples at various jet velocities. Increasing the sand concentration resulted in an initial increase in the surface roughness of the samples followed by a decrease at the higher sand concentrations. At a jet velocity of 9 m/s, the maximum surface roughness for both erosion and erosion-corrosion samples occurred at a low sand concentration of 1 g/L. Adding 1 g/L SiO₂ particles in the solution has boosted the surface roughness from a value of 0.12 µm (in the flow corrosion, i.e., with 0 g/L sand concentration) to 0.64 µm. Further increase in the sand concentration lowered the surface roughness to a value of about 0.3 µm at sand concentration of 90 g/L.

Comparing the surface roughness of the alloy at two jet velocities of 6 and 9 m/s in Fig. 2 revealed that the maximum surface roughness (R_a) was shifted from sand

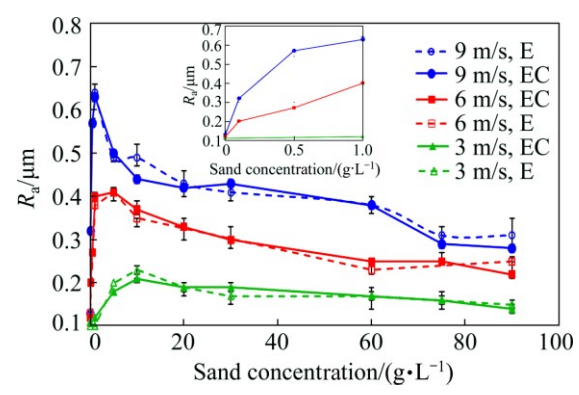


Fig. 2 Average roughness (R_a) values of eroded surfaces of Al-brass alloy after erosion (E) and erosion—corrosion (EC) tests at three jet velocities of 3, 6 and 9 m/s as function of particle concentration under impingement angle of 90°

concentration of 1 g/L at jet velocity of 9 m/s to 5 g/L at jet velocity of 6 m/s. Figure 2 also shows that there was a little change in the surface roughness of the alloy at a jet velocity of 3 m/s with sand concentration. This could be related to the very low energy of the impacted sands at this velocity, which resulted in a low plastic deformation on the surface. However, it could be stated that the sand concentration with the maximum R_a has increased to about 10 g/L for jet velocity of 3 m/s as compared to 6 and 9 m/s. The frequency of particle impingement, i.e., the number of particles impacting simultaneously on the surface decreased as the jet velocity was decreased. This means that at a particular sand concentration, the total particle impacts will be lower at a lower jet velocity. Therefore, a higher sand concentration would be needed to reach the maximum surface roughness at the lower jet velocities. Figure 2 also shows almost identical values of $R_{\rm a}$ on the erosion and erosion-corrosion samples at a particular jet velocity and a sand concentration. This might suggest that the electrochemical corrosion did not have any remarkable effect on the surface roughness (or surface deformation) of the eroded samples under an impingement angle of 90°.

Figure 3 shows the average roughness values of the eroded surface of Al-brass alloy after erosion and erosion–corrosion tests at three jet velocities of 3, 6 and 9 m/s as a function of particle concentration under an impingement angle of 40°. At jet velocities of 3 and 6 m/s, Fig. 3 shows that the surface roughness of eroded samples (E and EC) at impingement angle of 40° followed a same trend as was observed for impingement angle of 90° in Fig. 2. The maximum surface roughness of about 0.4 μ m (at sand concentration of 5 g/L) and 0.2 μ m (at sand concentration of 10 g/L) occurred under jet velocities of 6 and 3 m/s, respectively. At a jet velocity of 9 m/s, close values of R_a were obtained for the erosion–corrosion (EC) samples under impingement

angles of 40° and 90° at any sand concentration (Figs. 2 and 3). However, a different trend in the change in surface roughness with sand concentration was observed for the pure erosion (E) samples at a jet velocity of 9 m/s under an impingement angle of 40° compared with 90°. Figure 3 shows a same trend in R_a for the erosion and erosion-corrosion samples under impingement angle of 40° at sand concentrations up to 5 g/L with a peak at a sand concentration of 1 g/L at a jet velocity of 9 m/s. However, further increase in the sand concentration up to 30 g/L resulted in an increase and a decrease in the surface roughness of the erosion and erosion-corrosion samples, respectively. It was shown that the surface roughness of eroded samples reached almost constant values of about 0.78 and 0.38 µm on the erosion and erosion-corrosion samples, respectively.

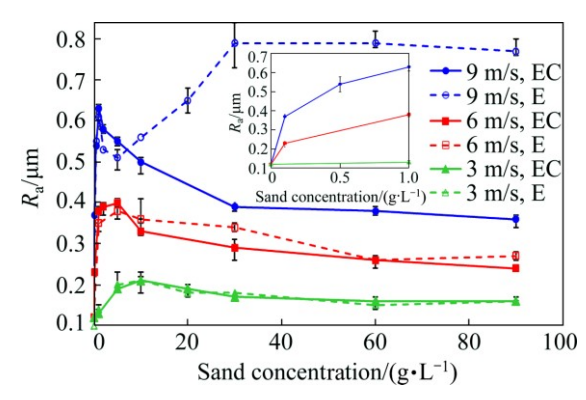


Fig. 3 Average roughness (R_a) values of eroded surfaces of Al-brass alloy after erosion (E) and erosion-corrosion (EC) tests at three jet velocities of 3, 6 and 9 m/s as function of particle concentration under impingement angle of 40°

Figures 2 and 3 also show that the surface roughness of the eroded samples has increased as the jet velocity was increased. This could be related to the higher energy of the impacted particles at the higher jet velocities, which induced more penetration and higher plastic deformation on the surface and resulted in a higher surface roughness. This point was also indicated by LOPEZ et al [1] who investigated the surface texture of AISI 304 and AISI 420 stainless steels after erosion—corrosion tests in a slurry pot tester.

The wear mechanisms that affected the surface roughness of samples during the erosion and erosion–corrosion tests under various test conditions could be characterized using SEM observations. SEM micrographs of the erosion–corrosion surfaces at a jet velocity of 9 m/s for various sand concentrations under two impingement angles of 90° and 40° are typically shown in Figs. 4 and 5, respectively. At low sand concentration of 0.1 g/L, Figs. 4(a) and 5(a) show a few erosive features on the eroded surfaces, which was probably caused by single impacts. The major features

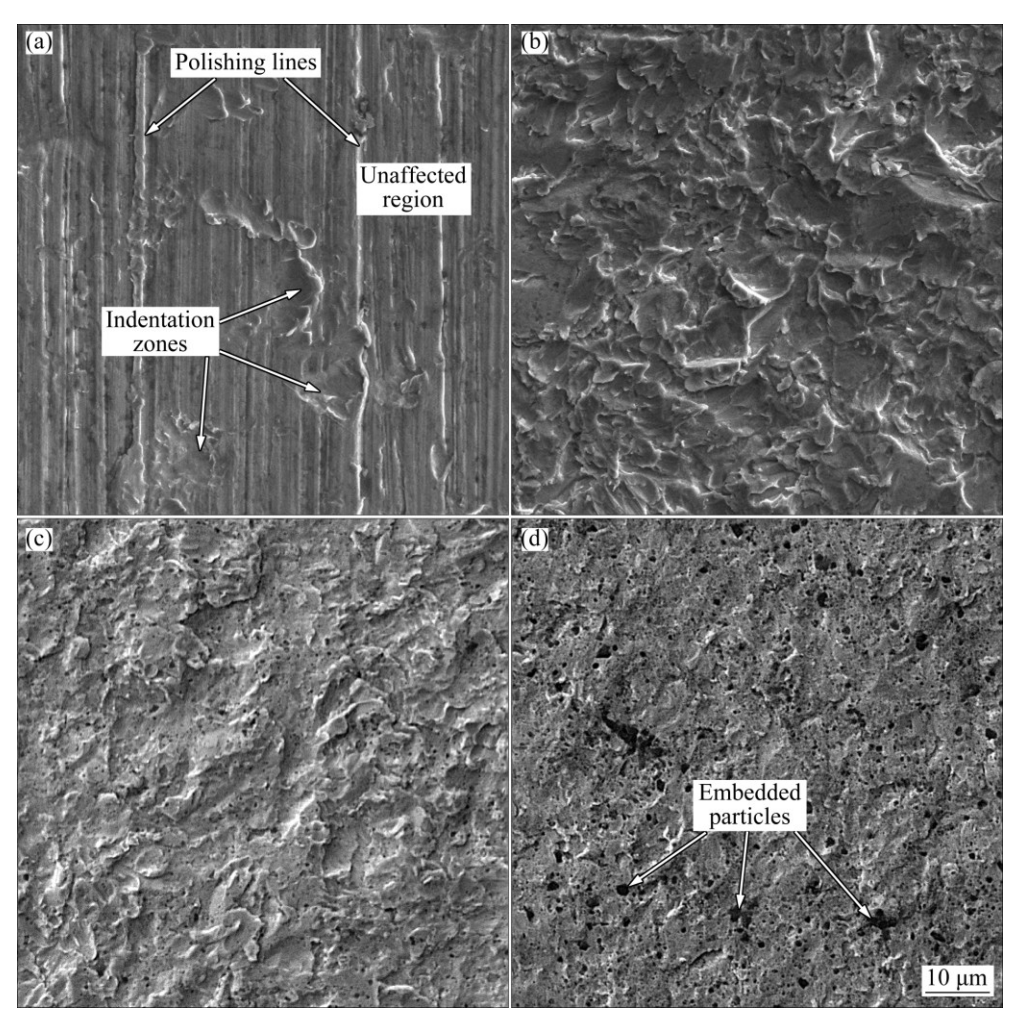


Fig. 4 SEM images of erosion–corrosion surfaces of Al-brass alloy at jet velocity of 9 m/s, impingement angle of 90° and different sand concentrations: (a) 0.1 g/L; (b) 1 g/L; (c) 5 g/L; (d) 90 g/L

on the surfaces were indentation in the impacted regions and erosive wear tracks at impingement angles of 90° and 40°, respectively. The formation of these features together with the raised lips around the impacted zones increased the surface roughness of the eroded samples at sand concentration of 0.1 g/L as compared to 0 g/L in Figs. 2 and 3.

A remarkable point in the erosion–corrosion surfaces at the sand concentration of 0.1 g/L was the existence of some unaffected regions on the surfaces at both impingement angles. It seems that under this condition (i.e., 30 min erosion at low sand concentration of 0.1 g/L), the number of impacts during the tests was not high enough to erode the whole area of the samples, as the polishing lines could still be observed in Figs. 4(a) and 5(a). These no-impact regions could result in a lower surface roughness at sand concentration of 0.1 g/L compared to 1 g/L in Figs. 2 and 3 (i.e., R_a values of 0.3 and 0.6 μ m for sand concentrations of 0.1 and 1 g/L, respectively). This indicated the importance of the plastic deformation induced by the impacts on the surface

roughness values of the eroded samples.

Figures 4 and 5 also show that at sand concentration of 1, 5 and 90 g/L, the whole area of the eroded surface was affected by the impacts at both impingement angles of 90° and 40°. Moreover, comparing the eroded surfaces at two sand concentrations of 1 and 90 g/L revealed a surface containing larger and higher deformed lips at concentration of 1 g/L. This confirmed the higher surface roughness of the eroded surfaces at lower sand concentration of 1 g/L compared with 90 g/L in Figs. 2 and 3. The particle impacts could induce craters with raised lips around the impacted zones at the normal incident (Fig. 4(b)) or erosive wear tracks with raised lips in front of the tracks at the oblique angles (Fig. 5(b)). The subsequent impacts of the particles could result in more plastic deformation of the raised lips and finally, detachment of the deformed lips and material removal [14]. It could be suggested that at a high sand concentration, the number of particles, which simultaneously impacted on the surface, was high enough to limit the extension of the raised lips around

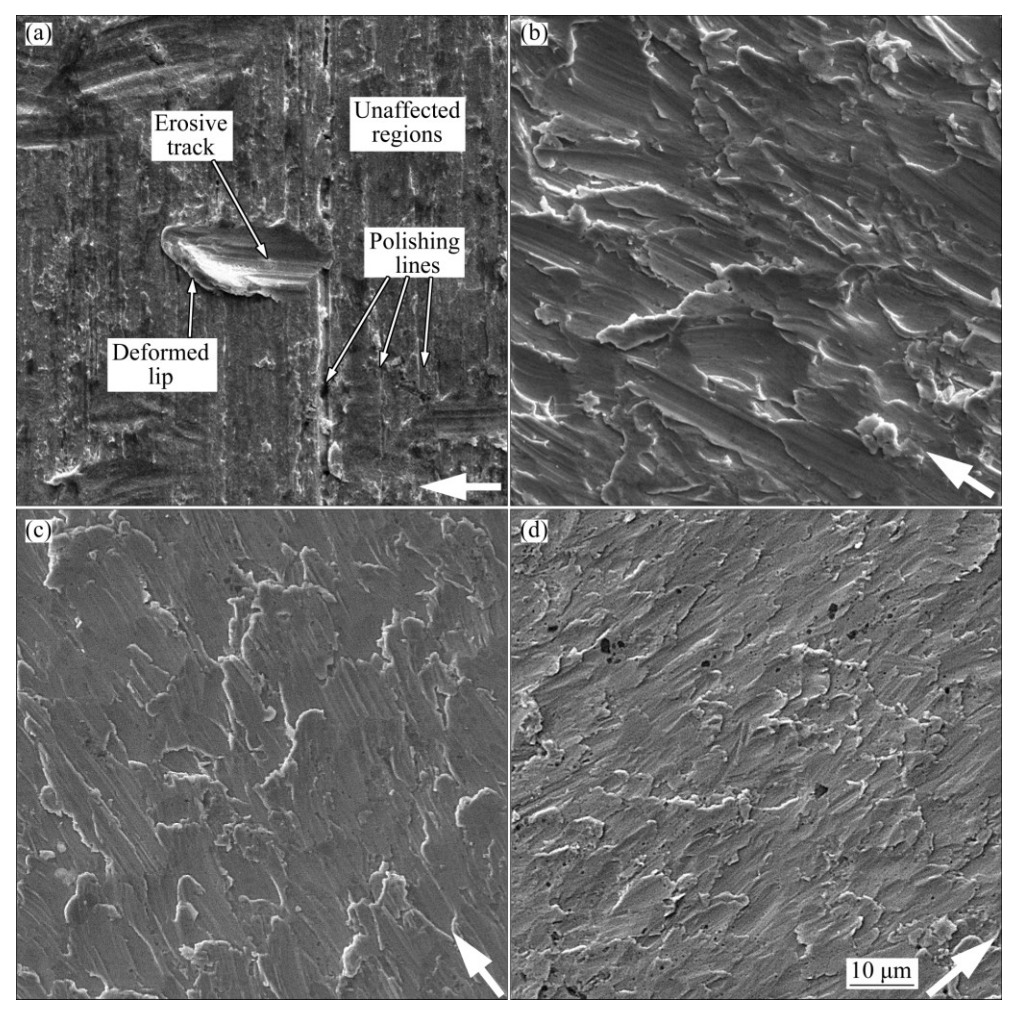


Fig. 5 SEM images of erosion–corrosion surfaces of Al-brass alloy at jet velocity of 9 m/s, impingement angle of 40° and different sand concentrations: (a) 0.1 g/L; (b) 1 g/L; (c) 5 g/L; (d) 90 g/L (Arrows in bottom right of images show erosion direction)

the impact zones. This could be a reason for the lower surface roughness of the samples at sand concentration of 90 g/L as compared to 1 g/L. Moreover, higher work-hardening of the surfaces at the higher sand concentrations could limit the plastic deformation of material on the eroded surfaces. This could also be resulted in the formation of the fine deformed lips on the eroded surfaces of the alloy at a sand concentration of 90 g/L in Figs. 4(d) and 5(d), leading to a lower surface roughness at the higher sand concentrations.

Rebounding or blanketing effect could also lower R_a values at the high sand concentrations. This effect has been considered to have an important role in reducing the erosion rate of various alloys at concentrated slurries [15–18]. After impinging of particles at high sand concentrations, they could rebound and generate a particle cloud on the surface and, therefore, protect the exposed surface against some of the subsequent incident particles [17]. The particle cloud might also decrease the energy transferred by the impacted particles on the surface, reduce the plastic deformation and the size of

deformed lips and, therefore, a lower surface roughness at the high sand concentrations. However, it should be mentioned that this effect would be more significant in determining the surface roughness of the alloy at impingement angle of 90° as compared with 40°.

EDS analysis of the eroded surfaces in Figs. 4 and 5 is given in Table 1. A higher content of silicon and oxygen was shown on the sample eroded at a sand concentration of 90 g/L as compared to 5 g/L, especially for impingement angle of 90°. This could be attributed to the embedding of larger number of SiO₂ particles on the eroded surface at a sand concentration of 90 g/L that was observed as dark regions in Fig. 4(d). The analysis of these regions is also given in Table 1. High amount of oxygen and silicon in the analysis of these regions confirmed the existence of SiO₂ particles embedded in these regions. Embedding of SiO₂ particles on the eroded surface of Al-brass alloy was previously studied in more details at a jet velocity of 6 m/s [14]. At impingement angle of 40°, Fig. 5 and Table 1 show a low amount of embedded particles on the eroded surface even at a sand

concentration of 90 g/L probably due to the low normal component of the particle velocity. However, Fig. 3 shows a decrease in $R_{\rm a}$ values of the erosion–corrosion surfaces at impingement angle of 40° with sand concentration. This might suggest that the embedding of erodent particles on the erosion–corrosion surfaces did not have a remarkable effect on the average surface roughness of the samples.

Table 1 EDS analysis result of eroded surfaces at jet velocity of 9 m/s shown in Figs. 4 and 5 (mass fraction, %)

Test condition	Cu	Zn	Al	О	Si
40°, 5 g/L	80.5	16.6	1.7	1.2	_
40°, 90 g/L	78.1	18.2	2.2	1.0	0.5
90°, 5 g/L	77.2	15.9	1.7	3.8	1.4
90°, 90 g/L	68.7	17.2	1.5	7.4	5.2
Dark region	36.8	8.1	0.1	31.9	23.1

In general, it could be suggested that work hardening, frequency of impacts and rebounding effect were the corresponding parameters in decreasing the surface roughness of the samples with sand concentration. The latter parameter had a lower effect on the surface roughness of the alloy at an impingement angle of 40°.

Figure 3 shows a deviation in the average surface roughness of the erosion and the erosion—corrosion

surfaces beyond the sand concentration of about 10 g/L at a jet velocity of 9 m/s under an impingement angle of 40°. Figure 6 shows low magnification SEM micrographs of both the erosion and the erosioncorrosion surfaces at a sand concentration of 90 g/L under an impingement angle of 40°. The corresponding surface roughness profiles are also presented in Fig. 6. Some well-defined ripples could be observed in SEM micrograph in Fig. 6(b) on the pure erosion sample. Figure 7 shows 3-D topography of the eroded surface after a pure erosion test at a jet velocity of 9 m/s, sand concentration of 90 g/L and an impingement angle of 40° for 30 min. The ripples were almost aligned perpendicular to the impact direction as could also be observed in the SEM image of the sample in Fig. 6(b). The corresponding roughness profile in Fig. 6(d) also illustrates the well-defined peaks and valleys of the ripples, 100 µm in wavelength and up to 4 µm in amplitude on the erosion surface. The ripple formation on surfaces of ductile materials during erosion process has also been reported in the literature [19-22]. However, no ripple pattern could be observed on the erosioncorrosion surface at sand concentration of 90 g/L and a jet velocity of 9 m/s in Fig. 6(a) and the corresponding surface roughness profile in Fig. 6(c). Any existence of the corrosion products or passive layers, i.e., copper oxides [23] on the erosion-corrosion surfaces could limit

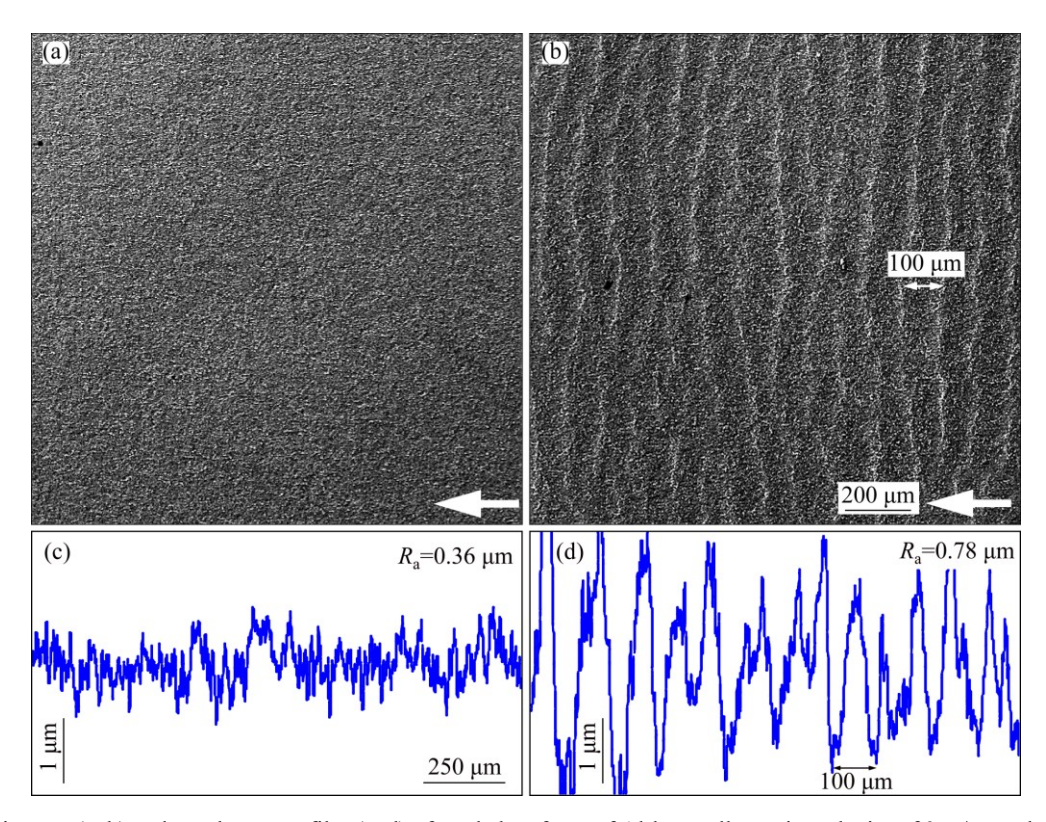


Fig. 6 SEM images (a, b) and roughness profiles (c, d) of eroded surfaces of Al-brass alloy at jet velocity of 9 m/s, sand concentration of 90 g/L and impingement angle of 40°: (a, c) Erosion-corrosion sample; (b, d) Erosion sample (Arrows in bottom right of SEM images show erosion direction)

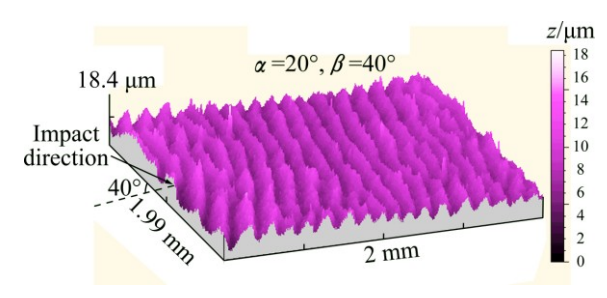


Fig. 7 3-D surface topography of Al-brass alloy after 30 min pure erosion test at jet velocity of 9 m/s, sand concentration of 90 g/L and impingement angle of 40° indicating formation of well-defined ripples

the deformation of the surface material by damping the energy of impacted particles required to plastically deform the eroded surfaces to allow the formation of ripples. Indeed, applying cathodic voltage of -1000~mV respect to OCP in the erosion tests could suppress the formation of the corrosion products and allow needed plastic deformation of the surface to form the ripples. The formation of ripples has significantly increased the average surface roughness of the erosion samples at a jet velocity of 9 m/s, impingement angle of 40° and sand concentrations higher than 10~g/L, as shown in Fig. 3.

Figure 8 shows the roughness profiles of the erosion samples at various sand concentrations at a jet velocity 9 m/s under an impingement angle of 40°. No ripple could be observed on the surfaces of erosion samples at two sand concentrations of 1 and 5 g/L. This resulted in a similar R_a for the erosion and erosion–corrosion samples at a jet velocity of 9 m/s in Fig. 3. Comparing the surface profiles at sand concentrations of 1 and 5 g/L revealed higher fluctuations with larger amplitude in the surface profile of sample at sand concentration of 1 g/L compared to 5 g/L. This was consistent with the larger surface features observed in SEM micrographs of the samples at sand concentration of 1 g/L in Fig. 5, which resulted in a higher surface roughness value at sand concentration of 1 g/L in Fig. 3. Well-defined ripple patterns could be observed in the roughness profile of the eroded surfaces at higher sand concentrations of 30 and 60 g/L in Fig. 8 as was observed for 90 g/L in Fig. 6(d). Therefore, the formation of ripples on the pure erosion samples at high sand concentrations was the main reason for the higher surface roughness of the erosion as compared with the erosion-corrosion samples at sand concentrations higher than 10 g/L in Fig. 3. It seems that a threshold sand concentration was needed to induce enough surface deformation on the erosion surfaces and form the ripple patterns. The dependence of ripple formation on the sand concentration was also mentioned by KARIMI and SCHMID [19].

Another point to be considered in Fig. 3 is that the

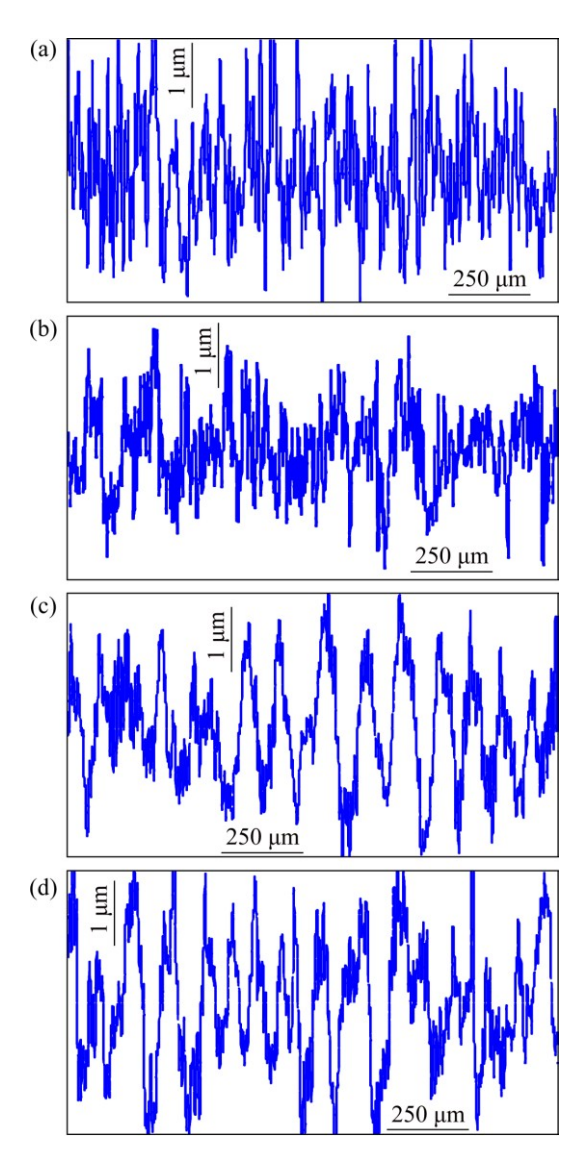


Fig. 8 Surface profiles of pure erosion samples of Al-brass alloy at jet velocity of 9 m/s, impingement angle of 40° and various sand concentrations: (a) 1 g/L; (b) 5 g/L; (c) 30 g/L; (d) 60 g/L

surface roughness profiles of both erosion and erosion—corrosion samples at jet velocities of 3 and 6 m/s followed a similar trend at various sand concentrations. The roughness profile observations indicated no ripple formation on the eroded surface of the alloy at these jet velocities even at a high sand concentration of 90 g/L. This revealed that the impact velocity (i.e., 9 m/s) or the energy of the particles was a very important parameter in the formation of the ripples on the eroded surfaces.

In order to investigate the effect of impingement angle on the surface roughness of the alloy, the variations of roughness of the eroded surfaces with impingement angle at a sand concentration of 60 g/L under three jet velocities of 3, 6 and 9 m/s were measured, as shown in Fig. 9. Impingement angle did not induce a remarkable change in the surface roughness of the alloy at jet

velocities of 3 and 6 m/s. Figure 10 shows the roughness profiles of the eroded surfaces at a sand concentration of 60 g/L under an impingement angle of 40° at two jet velocities of 3 and 6 m/s. Some larger wavelength and amplitude waves could be observed only on the surface profile under erosion at a jet velocity of 6 m/s in Fig. 10(d). They were considered as a part of the surface roughness and not a well-defined ripple with a larger repetitive wavelength and amplitude as was formed on the erosion surface at a jet velocity of 9 m/s in Fig. 8(d).

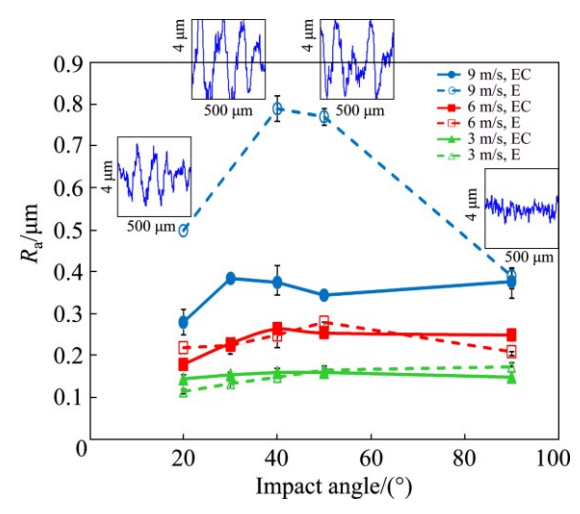


Fig. 9 Average roughness (R_a) values of erosion (E) and erosion—corrosion (EC) surfaces of Al-brass alloy at three jet velocities of 3, 6 and 9 m/s and sand concentration of 60 g/L as function of impingement angle

Figure 9 shows that the change in the surface roughness of the alloy with impact angle at a jet velocity of 9 m/s was also low in the erosion-corrosion condition. However, on the erosion samples, a significant change in the average surface roughness could be observed at a jet velocity of 9 m/s. The average R_a has increased from a value of 0.5 μm at impingement angle of 20° to 0.8 μm at impingement angle of 40°. Further increase in the impingement angle from 40° to 90° lowered the surface roughness to a value of about 0.4 μm . A part of the surface profile of the pure erosion samples at a jet velocity of 9 m/s is also shown in Fig. 9. At an impingement angle of 90°, the roughness profile indicated no ripple formation on the eroded surface probably due to higher surface work hardening, which resulted in a lower average roughness value as compared with the oblique angles. The roughness profiles showed that well-defined patterns in form of ripples were formed at oblique angles. However, comparing the surface profiles at oblique angles revealed a lower amplitude for the ripples at impingement angle of 20° compared with 40° and 50°, probably due to the lower normal component of the stress induced by the particles. The lower component of stress at impingement angle of 20°

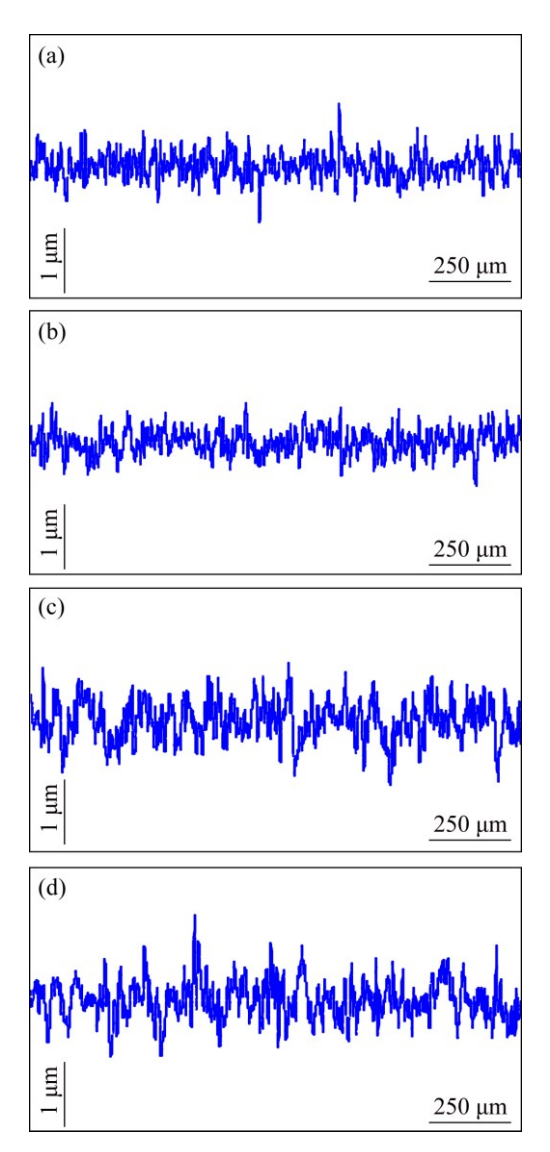


Fig. 10 Surface profiles of eroded surface of Al-brass alloy at sand concentration of 60 g/L under impingement angle of 40°: (a) EC sample, 3 m/s; (b) E sample, 3 m/s; (c) EC sample, 6 m/s; (d) E sample, 6 m/s

might cause less penetration of particle into the surface that could affect the amplitude of the ripples. Finer ripples (i.e., lower amplitude and shorter wavelength) formed on the erosion surface at impingement angle of 20° could be the main reason for the lower surface roughness of the eroded surface at this angle as compared with 40° and 50° in Fig. 9.

In general, the ripples could be formed on the eroded surface of Al-brass alloy in the following conditions: under pure erosion test, high jet velocity of 9 m/s, oblique angles and high sand concentrations. This caused a remarkable effect in the surface roughness of the alloy which may also affect the material removal mechanisms in the erosion process [5]. However, the findings of present work revealed that the ripples were not generated on the erosion—corrosion surfaces even at

high sand concentration of 90 g/L. This indicated the importance of electrochemical reactions on the mechanisms by which the ripples will form, a point which has not been considered in the literature.

4 Conclusions

- 1) The average surface roughness was increased with an increase in jet velocity. The change in the surface roughness with sand concentration and impingement angle was also higher at higher jet velocities.
- 2) The maximum roughness of the eroded surfaces at the jet velocity of 6 m/s occurred at a sand concentration of 5 g/L for both the erosion and erosion-corrosion tests at impingement angles of 40° and 90°.
- 3) At a jet velocity of 9 m/s and impingement angle of 90°, the maximum surface roughness was observed at a sand concentration of 1 g/L. A finer surface feature was observed on the eroded surfaces at the high sand concentrations. Work hardening, frequency of impacts and rebounding effect were considered as the corresponding parameters for the reduced surface roughness at the high sand concentrations.
- 4) At a jet velocity of 9 m/s and impingement angle of 40° , the surface roughness profile of the pure erosion and erosion–corrosion samples showed an opposite trend at sand concentrations higher than 10 g/L. In the erosion–corrosion samples, R_a showed a decrease with sand concentration, whereas, in the erosion samples, an increase in R_a with sand concentration was observed. The increase in R_a on the erosion surfaces was attributed to the formation of ripple that was confirmed by SEM and 3-D surface topography.
- 5) The formation of ripples on the pure erosion surfaces at a jet velocity of 9 m/s was also the main reason for the higher surface roughness of samples at the oblique angles as compared to the normal angle.

References

- [1] LOPEZ D, CONGOTE J P, CANO J R, TORO A, TSCHIPTSCHIN A P. Effect of particle velocity and impact angle on the corrosion–erosion of AISI 304 and AISI 420 stainless steels [J]. Wear, 2005, 259: 118–124.
- [2] ISLAMA M A, FARHAT Z N, AHMED E M, ALFANTAZI A M. Erosion enhanced corrosion and corrosion enhanced erosion of API X-70 pipeline steel [J]. Wear, 2013, 302: 1592–1601.
- [3] RAJAHRAM S S, HARVEY T J, WOOD R J K. Electrochemical investigation of erosion–corrosion using a slurry pot erosion tester [J]. Tribology International, 2011, 44: 232–240.
- [4] SASAKI K, BURSTEIN G T. The generation of surface roughness during slurry erosion-corrosion and its effect on the pitting potential [J]. Corrosion Science, 1996, 38: 2111–2120.
- [5] JAFARI M, MANSOORI Z, SAFFAR AVVAL M, AHMADI G. The effects of wall roughness on erosion rate in gas-solid turbulent

- annular pipe flow [J]. Powder Technology, 2015, 271: 248-254.
- [6] KANDLIKAR S G, JOSHI S, TIAN S. Effect of surface roughness on heat transfer and fluid flow characteristics at low Reynolds numbers in small diameter tubes [J]. Heat Transfer Engineering, 2003. 24: 4–16.
- [7] ZHENG Z B, ZHENG Y G, ZHOU X, HE S Y, SUN W H, WANG J Q. Determination of the critical flow velocities for erosion–corrosion of passive materials under impingement by NaCl solution containing sand [J]. Corrosion Science, 2014, 88: 187–196.
- [8] NGUYEN Q B, LIM C Y H, NGUYEN V B, WAN Y M, NAI B, ZHANG Y W, GUPTA M. Slurry erosion characteristics and erosion mechanisms of stainless steel [J]. Tribology International, 2014, 79: 1–7.
- [9] JI X, YANG S, ZHAO J, YAN C, JIANG L. Effect of heat treatment on slurry erosion wear resistance of amorphous Ni-P electrodeposits [J]. Tribology Transactions, 2012, 55: 86–90.
- [10] RYL J, DAROWICKI K, SLEPSKI P. Evaluation of cavitation erosion-corrosion degradation of mild steel by means of dynamic impedance spectroscopy in galvanostatic mode [J]. Corrosion Science, 2011, 53: 1873–1879.
- [11] LI Si-rui, ZUO Yu. Erosion-corrosion behavior of Pd-Co and Pd-Cu films on 316L stainless steel in simulated PTA slurry environment [J]. Transactions of Nonferrous Metals Society of China, 2016, 26: 167-174.
- [12] JHA A K, BATHAM R, AHMED M, MAJUMDER A K, MODI O P, CHATURVEDI S, GUPTA A K. Effect of impinging angle and rotating speed on erosion behavior of aluminum [J]. Transactions of Nonferrous Metals Society of China, 2011, 21: 32–38.
- [13] SAYED S M, ASHOUR E A, YOUSSEF G I. Effect of sulfide ions on the corrosion behaviour of Al-brass and Cu10Ni alloys in salt water [J]. Materials Chemistry and Physics, 2003, 78: 825–834.
- [14] ABEDINI M, GHASEMI H M. Synergistic erosion–corrosion behavior of Al-brass alloy at various impingement angles [J]. Wear, 2014, 319: 49–55.
- [15] DESALE G R, GANDHI B K, JAIN S C. Slurry erosion of ductile materials under normal impact condition [J]. Wear, 2008, 264: 322-330.
- [16] LINDGRENA M, PEROLAINEN J. Slurry pot investigation of the influence of erodent characteristics on the erosion resistance of austenitic and duplex stainless steel grades [J]. Wear, 2014, 319: 38-48
- [17] TURENNE S, FISET M, MASOUNAVE J. The effect of sand concentration on the erosion of materials by a slurry jet [J]. Wear, 1989, 133: 95–106.
- [18] DASGUPTA R, PRASAD B K, JHA A K, MODI O P, DAS S, YEGNESWARAN A H. Effects of sand concentration on slurry erosion of steels [J]. Materials Transactions, 1998, 39: 1185–1190.
- [19] KARIMI A, SCHMID R K. Ripple formation in solid-liquid erosion [J]. Wear. 1992. 156: 33–47.
- [20] BALLOUT Y A, MATHIS J A, TALIA J E. Effect of particle tangential velocity on erosion ripple formation [J]. Wear, 1995, 184: 17-21.
- [21] ZU J B, BURSTEIN G T, HUTCHINGS I M. A comparative study of the slurry erosion and free-fall particle erosion of aluminum [J]. Wear, 1991, 149: 73–84.
- [22] TALIA J E, BALLOUT Y A, SCATTERGOOD R O. Erosion ripple formation mechanism in aluminum and aluminum alloys [J]. Wear, 1996. 196: 285–294.
- [23] BECCARIA A M, POGGI G. Behaviour of aluminium brass in sea water at various temperatures [J]. British Corrosion Journal, 1988, 23: 122–130.

铝黄铜的冲蚀和冲蚀-腐蚀:射流速度、 石英砂浓度和撞击角对表面粗糙度的影响

Morteza ABEDINI^{1,2}, Hamid M. GHASEMI¹

- 1. School of Metallurgy and Materials Engineering, College of Engineering, University of Tehran, Tehran 11155-4563, Iran;
- 2. Department of Metallurgy and Materials Engineering, University of Kashan, Kashan, Iran

摘 要:研究射流速度、石英砂浓度和撞击角度对冲蚀和冲蚀-腐蚀后铝黄铜表面粗糙度的影响。冲蚀和冲蚀-腐蚀实验在射流冲击机中进行。采用二维和三维轮廓曲线仪以及扫描电子显微镜表征被侵蚀样品表面。结果表明,在9、6和3 m/s 射流速度下,分别增加石英砂浓度至1、5和10 g/L,冲蚀-腐蚀试样表面粗糙度增加;但是,进一步增加石英砂浓度,由于试样表面的加工硬化、反弹或覆盖效应以及高频冲击作用,试样表面粗糙度降低。随着射流速度的增加,试样表面粗糙度增加。研究结果还表明,当射流速度为3和6 m/s 时,试样表面粗糙度随撞击角度的变化并不明显;而在较高的射流速度9 m/s 时,倾斜撞击造成腐蚀表面形成波痕,因此,具有比正面撞击试样更高的表面粗糙度。

关键词: 铝黄铜; 侵蚀-腐蚀; 表面形貌; 石英砂浓度

(Edited by Bing YANG)